NASA Technical Memorandum 105972
AIAA–93–0173

Ice Accretion and Performance Degradation Calculations With LEWICE/NS

Mark G. Potapczuk
Lewis Research Center
Cleveland, Ohio

Kamel M. Al-Khalil
National Research Council
Washington, DC

and

Matthew T. Velazquez
Massachusetts Institute of Technology
Cambridge, Massachusetts

Prepared for the
31st Aerospace Sciences Meeting and Exhibit
sponsored by the American Institute of Aeronautics and Astronautics
Reno, Nevada, January 11–14, 1993

NASA

Ice Accretion and Performance Degradation Calculations with LEWICE/NS

Mark G. Potapczuk*
NASA Lewis Research Center, Cleveland, Ohio 44135

Kamel M. Al-Khalil†
National Research Council, Washington, D.C. 20418

Matthew T. Velazquez‡
Massachusetts Institute of Technology, Cambridge, MA 02139

Summary

The LEWICE ice accretion computer code has been extended to include the solution of the two-dimensional Navier-Stokes equations. The code is modular and contains separate stand-alone program elements that create a grid, calculate the flow field parameters, calculate the droplet trajectory paths, determine the amount of ice growth, calculate aeroperformance changes, and plot results. The new elements of the code are described. Calculated results are compared to experiment for several cases, including both ice shape and drag rise.

Nomenclature

A^+ = *26*
A_p = *Droplet surface area*
c_p = *Specific heat*
C_d = *Drag coefficient*
C_1 = *5*
C_2 = *2000*
$\vec{D}$ = *Drag*
$\hat{E}$ = *Convective flux terms in ξ-component of momentum equation*
E_m = *Total collection efficiency*
f = *Freezing fraction*
$\hat{F}$ = *Convective flux terms in η-component of momentum equation*
g = *Gravitational constant*
h_c = *Convective heat transfer coefficient*
i = *enthalpy*
J = *Jacobian of coordinate transformation*
k_s = *Roughness height*
L_f = *Heat of freezing*
L_v = *Heat of vaporization*
$\boldsymbol{l}$ = *Mixing length*
m = *Mass*
$\hat{Q}$ = *Solution matrix*
q = *Heat transfer*
r_c = *Recovery factor*
$\hat{S}$ = *Viscous flux terms in Navier-Stokes equation*
s = *Surface distance*
T = *Temperature*
u_τ = *Sheer velocity*
V = *Velocity, Volume*
x = *Spatial coordinate*
y = *Spatial coordinate*
α = *Angle of attack*
β = *Local collection efficiency*
κ = *Clauser constant, 0.0168*

---

* Aerospace Engineer, Member AIAA

† NRC Research Associate at NASA Lewis Research Center, Member AIAA

‡ Undergraduate Student

μ_t = *Eddy viscosity*
ν = *Kinematic viscosity*
ρ = *Density*
η = *Transverse coordinate in body-fitted system*
ξ = *Stream-wise coordinate in body-fitted system*

Subscripts

a = *Air*
c = *Convection, Incoming from cloud*
e = *Evaporation, Edge of boundary layer*
i = *Ice*
k = *Conduction*
o = *Release plane of water droplets*
p = *Particle (i.e. water droplet)*
r = *Runback*
s = *Static*
sur = *Surface*
v = *Vapor*
w = *Water*
∞ = *Free stream conditions*

I. Introduction

Over the past several years the need for ice accretion prediction capabilities has been growing. Many aircraft and ice protection system manufacturers have used the NASA developed ice accretion code, LEWICE.[1] The LEWICE code predicts the growth of ice on 2D surfaces through application of an inviscid panel method module, a particle trajectory calculation module, and a control volume energy balance/ice growth calculation module. The use of this code assists the analyst in assessment of potential icing hazards due to ice growth on unprotected surfaces and in the appropriate placement of candidate ice protection systems. Several upgrades to this code are currently underway to improve the capability of LEWICE. Some of these include; extension to 3D geometries,[2] inclusion of a thermal ice protection system model,[3] and the addition of a performance degradation evaluation capability.[4]

An additional area of potential improvement for the LEWICE code comes from the introduction of an alternate flow code calculation method. The current LEWICE code uses the inviscid panel method, S24Y, developed by Hess and Smith.[5] This approach has the advantage of being a very fast code and produces good results over an adequate range of conditions. There are several problems associated with the use of this code which have been documented in the LEWICE User's Manual[1] and by other users of the code.[6] The S24Y code uses a Karmen-Tsien compressibility correction. This helps extend the range of applicability to higher Mach numbers. However, the basis for this correction is a small perturbation approximation, hence thick airfoils and high angles of attack may not be accounted for using the correction. Additionally, the convective heat transfer values, which contribute significantly to the energy balance/ice growth calculation, may be quite different under conditions of high Mach number or of large local pressure gradients due to surface curvature.

Another area of concern is the evaluation of velocities near the surface at panel edges. The calculated velocities at the panel edges can become much larger than actual values, resulting in the possibility of unrealistic reversals in water droplet trajectories. This problem has been addressed in the LEWICE code by the creation of an artificial surface located some distance upstream of the actual surface. The droplets, now avoiding the flow reversals, impinge on this pseudo-surface and the local collection efficiency is calculated based on this surface.

The collection efficiency value is a measure of the amount of water impinging on the surface compared to the amount of water passing through a plane upstream of the airfoil bounded by the air-

foil thickness. The local collection efficiency is a measure of how droplet impingement varies along the surface of the airfoil. The local collection efficiency is based on an evaluation of the droplet impingement pattern as a function of distance along the surface. Thus, the pseudo-surface approximation can markedly change the collection efficiency values if it differs significantly from the actual surface contours. This has the potential for problems when determining the collection efficiency on iced surfaces.

In order to include more accurate velocity results near the airfoil surface and to include the effects of compressibility, the inviscid panel method was replaced by an Euler code. The use of an Euler code in place of the panel code in LEWICE was documented in a previous article.[7] This change also requires the use of a grid generator and the particle trajectory calculation must be altered to use interpolated velocities from a grid as opposed to determining the velocities by evaluating the contribution of each panel to the potential function at the desired location. The grid generator used has the ability to develop body-fitted grids for extreme shapes, such as glaze ice horns. The velocity interpolation calculation is incorporated into a subroutine within the particle trajectory code module.

Due to the irregular shapes associated with ice formations, multiple stagnation points can develop on the iced surface. This can lead to difficulty in selecting the point at which to start the boundary layer calculations for the upper and lower surfaces. LEWICE deals with this situation by either asking the user to select one of the stagnation points to start the boundary layer calculations or to create another pseudo-surface encompassing the stagnation points and calculating a single new stagnation point for that surface. The use of a grid based code can lead to different approaches to the solution of this problem. For example, the velocities at grid point locations away from the surface could be used to determine which grid line divides the upper surface from the lower surface and the surface point associated with that grid line could be the starting point for the boundary layer calculations. Such an approach could be automated and eliminate the need for user interaction as is currently the case in LEWICE. In this investigation, the point closest to the stagnation point from the previous time step is used to start the integral boundary layer calculation.

II. Code Description

The code consists of four major modules tied together by a simple command-line user interface. The four code modules are a grid generator, an Euler/Navier-Stokes flow solver, a particle trajectory calculation, and an energy balance/ice growth calculation. The code modules produce graphs of pressure coefficient distributions, lift and drag coefficient histories, residual histories, particle paths, collection efficiency distributions, flow field properties at the edge of the boundary layer, thermal conditions on the surface and the calculated ice shape. Contour plots can be produced which show the conditions in the far field. Output listings from each of the modules are also produced in order to allow examination of exact numerical values for parameters of interest. Files for geometry and flow solution information are written in PLOT3D[8] format in order to allow compatibility with other grid generators and flow solvers which could be substituted for those used in this code.

II-1. Grid Generation Module

The grid generator used in LEWICE/NS is a hyperbolic equation solver developed by Barth.[9] This code creates a C-grid around the user defined surface and can be easily applied to complex

surfaces such as an iced airfoil. The number of grid points and grid point spacing along the surface can be adjusted to concentrate grid points in regions of high curvature. This gives the user considerable flexibility in trying to develop an acceptable grid. An example of the grid generator output is shown in Figure 1, the grid for an iced NACA0012 airfoil.

The equations solved in this grid generator are hyperbolic and take the form;

$$x_\xi x_\eta + y_\xi y_\eta = 0 \qquad \text{Eq. 1}$$

$$x_\xi y_\eta - x_\eta y_\xi = \frac{1}{J} = V \qquad \text{Eq. 2}$$

where x and y are the Cartesian coordinates and ξ and η are the coordinates of the body-fitted system. The inverse of the Jacobian, J, approximates the local cell volume, V. Since this is a set of hyperbolic equations, they are solved using a marching procedure starting at the body surface and moving along the η direction out to the outer boundary.

One reason for choosing this grid generator is that it has been modified to work for surfaces with concave curvature or surface slope discontinuities. This is especially helpful when trying to regrid the geometry after the ice shape has been added. This grid generator has been used on several complex shapes as documented by Barth.[9] It has also been used extensively[2,7,12] for ice accretion geometries and has produced usable grids, for most cases with minimal user interaction. The issue of grid spacing in conjunction with the accuracy of the flow solution can be a problem even for clean airfoil geometries, however careful monitoring of the flow solution for decrease of the residuals, convergence of integrated results such lift, and development of inappropriate flow results (e.g. excessive entropy generation) should allow a high degree of confidence in the solution.

Since the overall LEWICE/NS code is modular, an alternate grid generator can be easily substituted for the current module. The only criterion for substitution is that the grid generator output the grid coordinates in PLOT3D format. This allows the grid file to be used by the other modules as well as by the PLOT3D visualization package.

II-2. Euler/Navier-Stokes Flow Solution Module

The Euler/Navier-Stokes code used in LEWICE/NS is the ARC2D code developed by Steger[10] and Pulliam.[11] This code uses the grid file and an input file which describes the flow conditions and selects some code procedure parameters. The code solves the Euler or Navier-Stokes equations in the body-fitted coordinate system. The equations solved are,

$$\partial_\tau \hat{Q} + \partial_\xi \hat{E} + \partial_\eta \hat{F} = Re^{-1} \partial_\eta \hat{S} \qquad \text{Eq. 3}$$

where the details of the terms in the equations can be found in references 10 and 11. The Cartesian coordinates (x,y) and the body-fitted coordinates (ξ,η) are obtained from the grid generator. Details of the numerical algorithm used to solve these equations are also found in references 10 and 11.

In addition to the flow solver, a turbulence model must also be used when the code is run in the Navier-Stokes mode. The turbulence model currently used in ARC2D for icing calculations is an

algebraic eddy viscosity model developed by Potapczuk.[12] This model does not require the determination of the boundary layer edge as in the Cebeci-Smith model nor does it require the determination of values along grid lines as in the Baldwin-Lomax model. This model is based on the mixing length concept and defines the eddy viscosity through appropriate length and velocity scales. In this model, the eddy viscosity, μ_t, is given by the equation,

$$\mu_t = \rho \boldsymbol{l}^2 |\omega| \qquad \text{Eq. 4}$$

In this model, the length scale is determined by the conditions at the surface and then saturates at some distance from the surface as indicated in the data of Klebanoff.[13] Hence, the length scale is given by the relation,

$$y^+ < C_1 \qquad \boldsymbol{l}(y) = \kappa \frac{C_1}{C_2} y^* \left(1 - \left(1 - \frac{y^+}{C_1}\right)^{C_2}\right)\left(1 - e^{-(y^+/A^+)}\right) \qquad \text{Eq. 5}$$

and,

$$y^+ > C_1 \qquad \boldsymbol{l}(y) = \kappa \frac{C_1}{C_2} y^* \qquad \text{Eq. 6}$$

where the constants C_1 and C_2 are determined empirically by matching the μ_t and $\boldsymbol{l}$ contours, for flat plate turbulent boundary layers, from the calculations with experimental results (normally C_1 = 5 and C_2 = 2000). The above equations include the terms y^* and y^+ which are measures of the transverse dimension within the boundary layer and are defined as,

$$y^+ = y/y^* \qquad \text{Eq. 7}$$

where,

$$y^* = \left.\frac{\nu}{\sqrt{|\tau|/\rho}}\right|_w \qquad \text{Eq. 8}$$

and where τ is the shear stress at the wall.

The mixing length and vorticity can be determined for any grid point with no need to march out from the surface along grid lines.

In addition to the turbulence model, a method of modeling roughness must be added to this calculation. The rough surfaces of an ice shape can cause premature transition from laminar to turbulent flow. This in turn can alter the drag and heat transfer characteristics of the iced airfoil. The Cebeci-Chang[14] model was chosen for use with ARC2D along with the turbulence model described above. The Cebeci-Chang model represents the roughness as a displacement to the bound-

ary layer that is factored into the calculation of the mixing length. The amount of the displacement, Δy, is based on the roughness height k_s and is calculated from the relation

$$\Delta y^+ = \begin{cases} 0.9\left[\sqrt{k_s^+} - k_s^+ \exp\left(\frac{-k_s^+}{6}\right)\right] & 5 < k_s^+ \le 70 \\ 0.7\,(k_s^+)^{0.58} & 70 \le k_s^+ \le 2000 \end{cases} \qquad \text{Eq. 9}$$

where $\Delta y^+ = \Delta y u_\tau / \nu$ and $k_s^+ = k_s u_\tau / \nu$.

The mixing length is then found by adding Δy into Eqs. 5 and 6. This produces the following equations.

$$\frac{y+\Delta y}{y^*} < C_1 \qquad \boldsymbol{l}(y) = \kappa \frac{C_1}{C_2} y^* \left(1 - \left(1 - \frac{\left(\frac{y+\Delta y}{y^*}\right)}{C_1}\right)^{C_2}\right)\left(1 - e^{-\left(\frac{y+\Delta y}{y^*}/A^+\right)}\right) \qquad \text{Eq. 10}$$

and,

$$\frac{y+\Delta y}{y^*} > C_1 \qquad \boldsymbol{l}(y) = \kappa \frac{C_1}{C_2} y^* \qquad \text{Eq. 11}$$

The velocity and pressure values resulting from the flow field calculation are used for several purposes in the LEWICE/NS code. They contribute to the evaluation of the particle trajectories. The values at grid lines away from the surface are used in the determination of boundary layer edge conditions. These edge values are used in the integral boundary layer calculation of the energy balance/ice growth module. Finally, the velocity and pressure field is used to determine the lift and drag values for the iced airfoil following the ice growth calculation.

The user determines the validity of the flow field solution by examining residual and lift histories and the pressure coefficient distribution and entropy contours. The flow field solution values are contained in the $\hat{Q}$ matrix, which is stored in PLOT3D format for plotting and to insure a standard file transfer process.

Normally, the flow solver is used in Euler mode during the ice accretion portion of the calculation. This allows the code to be run in a faster manner due mostly to the fewer number of grid points. There are some conditions for which the Navier-Stokes solution is required. This usually occurs when there are regions of high surface curvature resulting in large pressure gradients. These large gradients can result in convergence problems with the Euler equations. The viscous terms in the Navier-Stokes equations can introduce sufficient dissipation to allow convergence.

Once the final ice shape has been determined, the flow solver can be run again with the viscous terms included. This calculation provides information on the changes in lift and drag as a result of

the ice shape. This usually requires the use of the grid generator again in order to develop a grid of sufficiently fine resolution to capture the flow gradients near the surface.

II-3. Particle Trajectory Module

Once the flow field for a given geometry has been obtained, the velocities are used to determine the trajectories of super-cooled water droplets from release points upstream of the body to impact locations on the surface. In the original LEWICE code, this was done with a Lagrangian predictor-corrector method in a code developed for LEWICE.[1] This code is also used for LEWICE/NS, however, some changes were required in order to deal with a grid-based flow code instead of the original inviscid panel method, which can determine velocity values at any arbitrary location.

The equations of motion for water droplets are based on the assumption that they are rigid spheres and hence the only forces acting are drag and gravity. This assumption is considered valid for droplet radii of less than 500 μm.[1] The governing equations are thus,

$$m\ddot{x} = -\vec{D}\cos\gamma + mg\sin\alpha$$
$$m\ddot{y} = -\vec{D}\sin\gamma - mg\cos\alpha \qquad \text{Eq. 12}$$

where

$$\gamma = \tan^{-1}\frac{\dot{y}_p - V_y}{\dot{x}_p - V_x} \qquad \text{Eq. 13}$$

$$\vec{D} = C_d\frac{\rho_a V^2}{2}A_p \qquad \text{Eq. 14}$$

$$V = \sqrt{(\dot{x}_p - V_x)^2 + (\dot{y}_p - V_y)^2} \qquad \text{Eq. 15}$$

and where V_x and V_y are the components of the flow field velocity at the droplet location and $\dot{x}_p$, $\dot{y}_p$, $\ddot{x}_p$ and $\ddot{y}_p$ are the components of the droplet velocity and acceleration, respectively.

The water droplet trajectories are calculated using an Adams-Boulter predictor-corrector algorithm. After each calculation of a droplets location, it is checked to determine if it has impacted on the body. The calculation continues until a droplet impacts the surface or until it has passed some user selected location, indicating that the droplet has missed the body. Details of this calculation are found in reference 1.

As mentioned in the introduction, the original LEWICE code requires a pseudo-surface in order to avoid unrealistic velocities near the surface which lead to inaccurate droplet trajectories. The use of a grid based code avoids this problem. Any inviscid flow solution does require some special treatment near the surface. The slip flow at the surface is not physically correct and thus the droplet trajectory calculation does not use those values. Instead, once the particle has crossed the first

grid line off of the surface, the droplet path is no longer altered by the flow field and is considered to be tangent to the previously calculated path line. The intersection of that path line with the body surface is taken as the impingement location.

The pattern of droplet impingement on the body surface determines the amount of water that hits the surface and becomes part of the ice growth process. The ratio of the actual mass that impinges on the surface to the maximum value that would occur if the droplets followed straight-line trajectories, is called the total collection efficiency, E_m. The total collection efficiency for the body is found by integrating the local collection efficiency, β, between the upper and lower limits of droplet impingement. The local collection efficiency is defined as the ratio, for a given mass of water, of the area of impingement to the area through which the water passes at some distance upstream of the airfoil. Taking a unit width as one dimension of both area terms, the local collection efficiency can then be defined as,

$$\beta = \frac{dy_o}{ds} = \frac{\Delta y_o}{\Delta s} \qquad \text{Eq. 16}$$

where Δy_o is the spacing between water droplets at the release plane and Δs is the distance along the body surface between the impact locations of the same two droplets. The local collection efficiency is illustrated in Figure 2.

The local collection efficiency is the necessary input for the energy balance/ice growth module. It, along with the free stream velocity and the cloud liquid water content, determines how much water impinges on the local region of the surface under consideration. Variations in the local collection efficiency can significantly alter the ice growth for that surface region.

II-4. Energy Balance/Ice Growth Module

The growth of ice on the surface is a complex fluid dynamics, heat transfer, and mass transfer process. The incoming water may freeze on impact or some fraction may freeze while the remaining water either runs along the surface or collects in pools. The processes determining which of these occur include surface tension effects, roughness, skin friction between water and ice or water and airfoil surface, shear forces between water and air, and convection and conduction heat transfer. A simplified model of this process has been developed by Messinger[15] and is used in the original LEWICE code. This model is used in the LEWICE/NS model as well. However, as alternate ice growth models are developed, they may easily be substituted into this code due to its modular nature.

The Messinger model, as implemented in the LEWICE code, is described fully in Appendix A of the LEWICE User's Manual.[1] As such, only a brief description will be given here. The ice growth process is modeled as a control volume analysis. The control volume is bounded by the body surface and by an arbitrary boundary considered to be at the edge of the boundary layer. The two chordwise boundaries coincide with constant ξ grid lines established by the grid generation code. The lower boundary of the control volume is initially the body surface but it moves outward with the ice growth process, remaining at the top of the solid-fluid interface. For dimensional completeness, the control volume is considered to extend one unit length in the spanwise direction.

The control volume is used to perform a mass and energy balance, as depicted in Figures 3 and 4. The equation governing the mass balance is,

$$\dot{m}_c + \dot{m}_{r_{in}} - \dot{m}_e - \dot{m}_{r_{out}} = \dot{m}_i \qquad \text{Eq. 17}$$

where $\dot{m}_c$ is mass flow rate of incoming water, $\dot{m}_{r_{in}}$ is the mass flow rate of runback water from the previous control volume, $\dot{m}_e$ is the mass flow rate of evaporated water, $\dot{m}_{r_{out}}$ is the mass flow rate of water running back to the next control volume, and $\dot{m}_i$ is the mass flow rate of water leaving the control volume due to freeze-out. The equation governing the control volume energy balance is,

$$\begin{aligned} &\dot{m}_c i_{w,T} + \dot{m}_{r_{in}} i_{w,sur\,(i-1)} \\ &= (\dot{m}_e i_{v,sur} + \dot{m}_{r_{out}} i_{w,sur} + \dot{m}_i i_{i,sur} + q_c \Delta s + q_k \Delta s) \end{aligned} \qquad \text{Eq. 18}$$

where $i_{w,T}$ is the stagnation enthalpy of the incoming water droplets, $i_{w,sur\,(i-1)}$ is the enthalpy of the water flowing into the control volume from upstream, $i_{v,sur}$ is the enthalpy of the vapor leaving the control volume due to evaporation, $i_{w,sur}$ is the enthalpy of the water running back to the next control volume, $i_{i,sur}$ is the enthalpy of the ice leaving the control volume, q_c is the heat transfer due to convection, and q_k is the heat transfer due to conduction at the bottom of the control volume.

The incoming energy due to water droplet impingement and runback are calculated from known information. The energy leaving the control volume due to evaporation and convection can be calculated independently. Currently, the convection heat transfer calculation is performed in the same manner as in the original LEWICE code. That is, an integral boundary layer analysis is performed using the Euler calculation results as the boundary layer edge conditions. The code could be used in Navier-Stokes mode to obtain these values, but the integral boundary layer calculation is faster and thus was used in this investigation. The heat transfer due to conduction is not considered in this analysis, as the ice layer is considered to act as an insulating surface. This leaves the energy loss due to freeze-out and the energy leaving the control volume due to runback as unknowns. In particular, the mass flow rates for these two terms are unknown, as was the case for the mass balance. This leaves two equations and two unknowns and the system can be solved. The details of the evaluation of each of the terms in the energy equation can be found in Appendix A of the LEWICE User's Manual.[1]

A useful concept for evaluation of the nature of the ice accretion being calculated is the freezing fraction. This is the fraction of the total water coming into the control volume that changes phase to ice. The equation defining freezing fraction is,

$$f = \frac{\dot{m}_i}{\dot{m}_c + \dot{m}_{r_{in}}} \qquad \text{Eq. 19}$$

This term can also be used to simplify the evaluation of the energy balance.

The convection heat transfer term plays an important role in the LEWICE/NS energy balance. It is through this term that the aerodynamics and the roughness levels can influence the development of the ice accretion. Currently, the convection heat transfer is determined from an evaluation of the boundary layer growth on the surface, using an integral boundary layer method. The pressure distribution determined by the Euler calculation is used as input to the boundary layer calculation. The boundary layer calculation determines the displacement thickness and the momentum thickness. The Reynold's analogy is used to determine the heat transfer coefficient. Roughness is accounted for by a correlation developed by Ruff.[1] The complete description of the integral boundary layer calculation is found in Appendix B of the LEWICE User's Manual.[1]

Expanding the terms in the energy equation as described in the LEWICE manual and combining Eqs. 17-19 yields the following form of the energy equation,

$$\dot{m}_c\left[c_{p_{w,s}}(T_s - 273.15) + \frac{V_\infty^2}{2}\right]$$

$$+\dot{m}_{r_{in}}\left[c_{p_{w,sur(i-1)}}(T_{sur(i-1)} - 273.15)\right] + q_k \Delta s$$

$$= m_e\left[c_{p_{w,sur}}(T_{sur} - 273.15) + L_v\right]$$

$$+\left[(1-f)(\dot{m}_c + \dot{m}_{r_{in}}) - \dot{m}_e\right] c_{p_{w,sur}}(T_{sur} - 273.15) \qquad \text{Eq. 20}$$

$$+f(\dot{m}_c - \dot{m}_{r_{in}})\left[c_{p_{i,sur}}(T_{sur} - 273.15) - L_f\right]$$

$$+h_c\left[T_{sur} - T_e - \frac{r_c V_e^2}{2c_{p_a}}\right]\Delta s$$

The solution process for this equation is started by identifying the stagnation point. Since no runback water can enter the control volumes on either side of the stagnation point, one of the unknowns is determined for these two control volumes. Thus, the solution may be marched back, on the upper and lower surfaces, towards the trailing edge from the stagnation point. As $\dot{m}_i$ is determined for each control volume, the resulting ice growth thickness can be found from the ice density and the dimensions of the control volume. The ice thickness values define a new iced airfoil geometry by adding that thickness to the body in a direction normal to the surface. In regions of high curvature, the new ice surfaces can intersect or diverge.The method for dealing with the redefinition of the surface under these circumstances is the same as that of the original LEWICE code and is described in Reference 1. Once the new geometry has been defined, the entire process can be started again at the grid generation step.

III. Comparison to measured ice accretion and drag

The LEWICE/NS code was used to calculate ice shapes on a NACA 0012 airfoil for a series of conditions tested by Olsen, et al,[16] in the NASA Lewis Icing Research Tunnel (IRT). In that test

program, the ice shapes and resulting drag values were measured for a series of tests on the NACA 0012 airfoil with varying icing conditions. The code was used to try and reproduce the results of the test for both ice shape and drag.

III-1. Ice shape predictions

The Olsen tests covered a wide range of conditions and examined such effects as temperature, drop size, and liquid water content (LWC). The most dramatic effect uncovered, with respect to drag, was the correlation of drag with temperature. Figure 5 shows the variation of drag as a function of temperature. At temperatures just below freezing, there is a large increase in drag which tapers off as the temperature decreases. The suspected reason for this is the change from a glaze ice condition to a rime ice condition. The glaze shapes, with their associated horns, cause a significant change to the pressure distribution over the airfoil resulting in the large change in drag. Rime ice, on the other hand, has a smaller effect on the pressure distribution with the drag rise being mostly due to skin friction.

This series of sixteen temperature conditions (with LWC $\times$ V $\times$ Time held constant) is detailed in Table 1. The LEWICE/NS code was used to evaluate these cases in order to evaluate its ability to predict ice accretion over a wide range of conditions. There were some difficulties in obtaining solutions for some of these cases. These problems were either with grid creation or with convergence of the flow field calculation. Further investigation is required in order to determine what steps need to be taken to overcome these difficulties. In all, eleven of the fourteen cases with ice depositions were calculated. Measured coordinates for two of these eleven were not available and so only nine cases were compared. The results of the LEWICE/NS analysis indicates reasonable agreement with the rime ice conditions and fair to poor agreement with the glaze ice conditions. Additionally, the transition from rime to glaze shapes appears to occur at different temperatures in the code results than in the experimental results. This can be seen in Figs. 6 and 7.

The differences between calculation and experiment can be attributed to two sources. The LEWICE/NS pressure distributions and droplet trajectories are not the same as those of the original LEWICE code. This was demonstrated in a previous investigation.[7] As a result, the distribution of incoming water on the surface is different between the two codes as is the convective heat transfer acting on that water. The differences in these two calculations leads to significant differences in the resulting ice shapes. The roughness correlation used in LEWICE, which has a significant effect on the convective heat transfer coefficient, was tuned to the LEWICE results in order to produce reasonably accurate ice shapes over a limited range of icing conditions. The results of this investigation indicate that the correlation is not appropriate for the LEWICE/NS code. This means that either a new correlation is required for the LEWICE/NS code or the convection heat transfer must be obtained from the energy equation directly. The former approach would require a parametric investigation over several icing cloud conditions, such as temperature, velocity, LWC, or droplet size, to determine correlations between input roughness levels and output ice shapes. In this approach, the development of a suitable correlation is dependent on how representative the correlating data set is of all possible icing conditions. However, it does have the advantage of producing satisfactory results over some range of conditions. The latter approach would necessitate the use of the viscous option in the LEWICE/NS code during each time step of the ice accretion calculation.

Without considering the correlation between prediction and experiment, there are some interesting features of the LEWICE/NS ice shape results which deserve further comment. In one case, shown in Fig. 8, the ice shape produces a shadow region for droplet impact. That is, a protuberance in the ice shape blocks water droplets from impacting on a portion of the surface aft of the protuberance. Droplets originating from points lower along the release plane do impact further aft on the surface, once they pass under the protuberance. This results in two distinct collection efficiency curves as seen in Fig. 9.

The convective heat transfer coefficient in this region is such that the freezing fraction is less than unity. This means that some of the water on the protuberance travels back into the region with no impingement. The water then rapidly freezes before traveling back to the region where impingement resumes. In the aft impingement region, the heat transfer is high enough to cause rapid freezing and a large horn develops in this region as seen in Fig. 6(c). This secondary horn is also evident in the experimental shape corresponding to this condition, albeit of smaller size. This interplay of collection efficiency and convective heat transfer is postulated to be a possible mechanism for the formation of ice fingers, seen frequently on actual ice shapes but never actually modeled. A similar horn is also seen in the Fig. 6(b), again for both the calculated and experimental results.

III-2. Iced airfoil drag predictions

Results from previous investigations by Shin, et al,[4] have indicated very good agreement between calculations and experimental values. Their calculations captured the large rise in drag at warm temperatures associated with glaze ice conditions. There were some differences in the level of drag which they associated with transition and roughness modeling. In a later investigation,[17] they were able to account for this difference by extending the rough region well beyond the ice growth region on the airfoil. In an effort to avoid using this artifice, the LEWICE/NS code is being used to examine the drag results of the calculated ice shapes described in the previous section.

Since many of the calculated ice shapes did not match the experimental values, especially for the glaze ice conditions, it was not expected that the resulting drag values would compare favorably. However, the drag values were evaluated in order to determine if the large drag rise at warm temperatures would be seen in the calculations. The drag value for these calculations were produced by using the standard LEWICE roughness value as the value for k_s used in Eq.9 (i.e. k_s = XKINIT). The k_s values used in the calculations are shown in Table 1. These roughness levels were applied only over the region with ice on the surface. A value of $k_s = 0.5 \times 10^{-5}$ was used in the clean region of the surface. This was done in order to simulate some minimal roughness level of a clean surface. The resulting drag values are shown in Fig. 5.

Drag calculations for glaze ice geometries have been calculated before using this roughness model.[12] The results have indicated that the pressure drag is a much more influential term than the viscous drag for glaze ice formations with substantial horn growths. As a result, it is expected that the drag predictions for rime ice formations will be more sensitive to the roughness and turbulence modeling described above.

The drag results parallel the ice shape results in terms of agreement with experimental values. The low speed results agree quite well with the measured drag values at low temperatures. At warmer temperatures, where the pressure component of the drag is predominant, the results do not compare as well. The agreement between calculated and measured ice shapes is also not that good at

these conditions. The high speed results do not agree as well as the low speed results. The drag is underpredicted at all temperatures. The drag values at warmer temperatures were not obtained for this velocity because of difficulties in determination of the final ice shape, as described previously. It can be seen, though, that even at -12°C the drag values begin to differ markedly between the calculation and experiment. Comparison of the ice shapes for this condition, Fig. 7(b), indicates that the experimental condition is a glaze formation while the calculated result is a rime shape. This explains the marked difference in drag results for this case. As a result of the difficulties in determining the ice shape for the warmer conditions, the ability of the code to reproduce the characterisitic drag rise could not be evaluated.

IV. Concluding Remarks

A new version of the LEWICE family of codes has been developed which substitutes the use of a Navier-Stokes code for the potential flow code, S24Y. The code is normally used in an Euler mode during the ice accretion portion of the calculation with the viscous terms added only during the follow-on performance degradation calculations. As documented previously,[7] the new code has the capability to calculate ice shapes for high Mach numbers and large angles of attack.

Comparisons of code results to experimental ice tracings were good for rime ice conditions but were only fair to poor for glaze ice accretions. The differences are considered to arise from poor correlation of the roughness parameter with the boundary layer edge velocity and pressure distributions calculated by the Euler portion of the code. Close correlation between the LEWICE code roughness parameter and the convective heat transfer coefficient was necessary to produce good agreement between ice accretion prediction results and actual ice tracings in the original LEWICE. This correlation will have to be adjusted to allow use of the Euler code within the LEWICE framework. Development of an alternate correlation suggests that some additional experimental data on heat transfer, collection efficiency, and roughness characterization for ice shapes would be useful for enhancing the robustness of any such correlation. An alternative would be to utilize the solution of the energy equation, obtained from a Navier-Stokes calculation prior to each ice accretion calculation time step, in place of the integral formulation currently found in LEWICE and LEWICE/NS. This latter approach may still require correlation information, however it may be on a lower level of approximation, such as the heat transfer coefficient over a characteristic roughness element. Further investigation of the relationship between roughness level and ice shape thus seems warranted no matter which approach is pursued.

Run No.	Air speed *km/hr*	Total Temp. *°C*	LWC g/m^3	DVM *μm*	Time *min*	Drag Coef. C_D	XKINIT = k_s
1	209	-2	1.3	20	8	0.02807	7.906×10^{-3}
2		-1				0.02647	8.168×10^{-3}
3		-5				0.06036	7.120×10^{-3}
4		-8				0.02949	6.334×10^{-3}
5		-18				0.02161	3.715×10^{-3}
6		-26				0.01941	1.619×10^{-3}
7		-15				0.02105	4.500×10^{-3}
8		-12				0.02072	5.309×10^{-3}
9		-20				0.01773	3.191×10^{-3}
10		0				0.00814	
11	338	-2	1.05		6.2	0.0756	8.109×10^{-3}
12		-8				0.0606	6.344×10^{-3}
13		-12				0.0370	5.167×10^{-3}
14		-17				0.0284	3.695×10^{-3}
15		-26				0.0238	1.048×10^{-3}
16		0				0.00814	

Table 1: Test Conditions for Icing Tests with NACA 0012 Airfoil, Chord = 0.53m, Angle of Attack = 4°

References

1. Ruff, G.A. and Berkowitz, B.M., "User's Manual for the NASA Lewis Ice Accretion Prediction Code (LEWICE)," NASA CR-185129, May 1990.
2. Potapczuk, M.G. and Bidwell, C.S., "Numerical Simulation of Ice Growth on a MS-317 Swept Wing Geometry," NASA TM-103705, AIAA Paper No. 91-0263, Jan. 1991.
3. Wright, W., DeWitt, K., and Keith, T., "Numerical Simulation of Icing, Deicing, and Shedding," AIAA Paper No. 91-0665.
4. Shin, J., Berkowitz, B., Alemdaroglu, N., and Cebeci, T., "Prediction of Ice Shapes and Their Effect on Airfoil Performance," AIAA Paper No. 91-0264, Jan. 1991.
5. Hess, J.L. and Smith, A.M.O., "Calculation of Potential Flow About Arbitrary Bodies," Progress in Aeronautical Sciences, Vol. 8, (ed. D. Kuchemann), Pergamon Press, Elmsford, NY, 1967, pp. 1-138.
6. Berkowitz, B.M. and Riley, J.R., "Analytical Ice Shape Predictions for Flight in Natural Icing Conditions," NASA CR 182234, Dec. 1988.
7. Potapczuk, M.G., "LEWICE/E: An Euler Based Ice Accretion Code," NASA TM 105389, AIAA Paper No. 92-0037, Jan. 1992.
8. Walatka, P.P., Buning, P.G., Pierce, L., and Elson, P.A., "PLOT3D User's Manual," NASA TM 101067, March 1990.
9. Barth, T., Pulliam, T.H., and Buning, P.G., "Navier-Stokes Computations for Exotic Airfoils," AIAA Paper No. 85-0109, Jan. 1985.
10. Steger, J.L."Implicit Finite Difference of Flow About Arbitrary Geometries with Application to Airfoils," AIAA Paper No. 77-665, 1977.
11. Pulliam, T.H., "Euler and Thin Layer Navier-Stokes Codes: ARC2D, ARC3D, Notes for Computational Fluid Dynamics User's Workshop, UTSI E02-4005-023-84, March 1984.
12. Potapczuk, M.G., "Navier-Stokes Analysis of Airfoils with Leading Edge Ice Accretions," Ph.D. Dissertation, The University of Akron, May 1989.
13. Klebanoff, P.S., NACA Report No. 1247, 1955.
14. Cebeci, T. and Chang, K.C., "Calculation of Incompressible Rough Wall Boundary Layer Flows," AIAA Journal, Vol. 16, No. 7, July 1978, pp. 730-735.
15. Messinger, B.L., "Equilibrium Temperature of an Unheated Icing Surface as a Function of Airspeed," Journal of Aeronautical Sciences, Vol. 20, No. 1, 1953, pp. 29-42.
16. Olsen, W., Shaw, R., and Newton, J., "Ice Shapes and the Resulting Drag Increase for a NACA 0012 Airfoil," NASA TM 83556, Jan. 1984.
17. Shin, J., Chen, H.H., and Cebeci, T., "A Turbulence model for Iced Airfoils and its Validation," NASA TM 105373, AIAA Paper No. 92-0417, Jan. 1992.

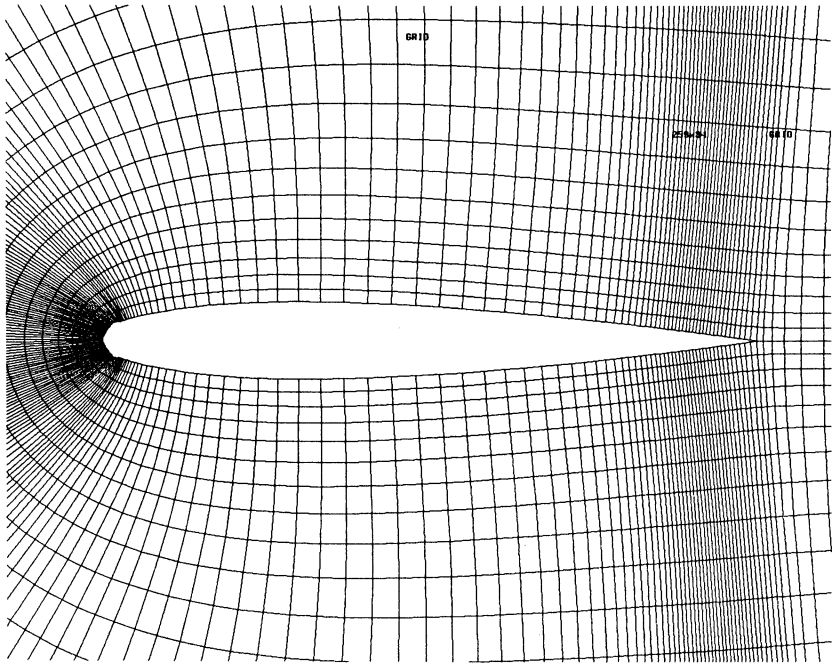

Figure 1 - Near field grid for NACA 0012 airfoil with ice shape on leading edge.

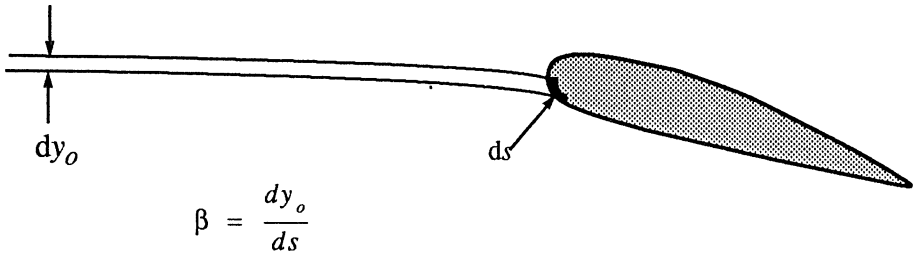

$$\beta = \frac{dy_o}{ds}$$

Figure 2 - Definition of local collection efficiency.

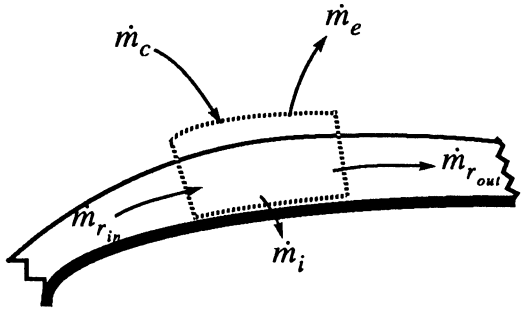

Figure 3 - Mass balance control volume.

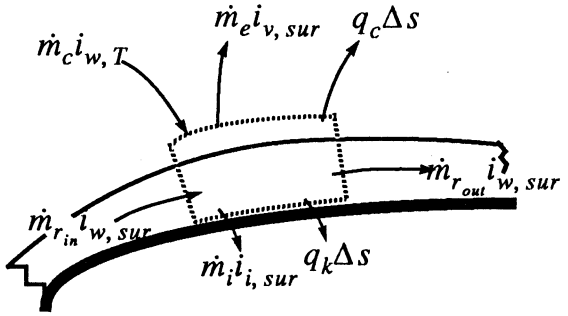

Figure 4 - Energy balance control volume.

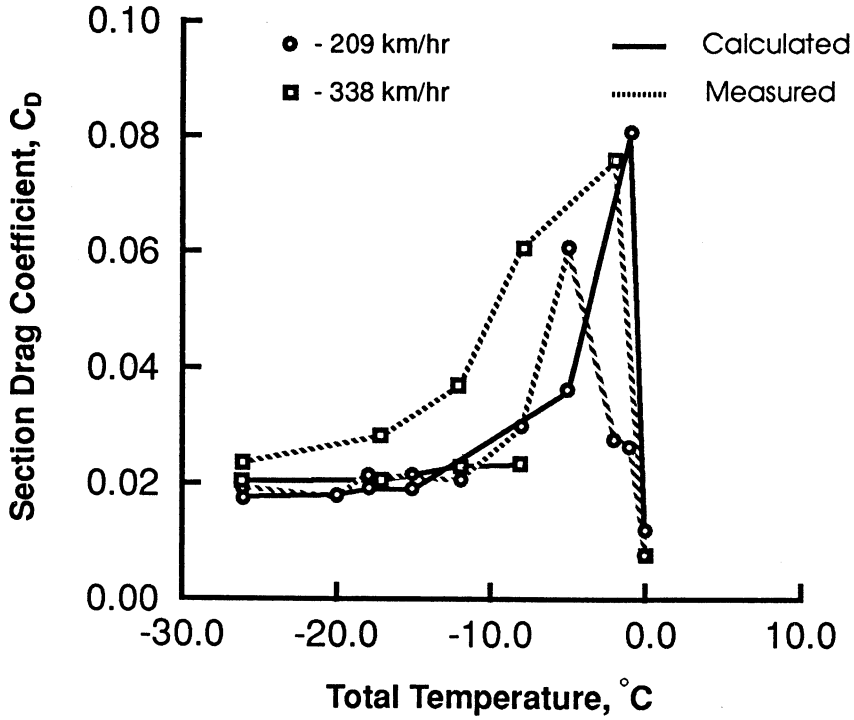

Figure 5 - Comparison of measured and calculated drag coefficent results for several temperature conditions

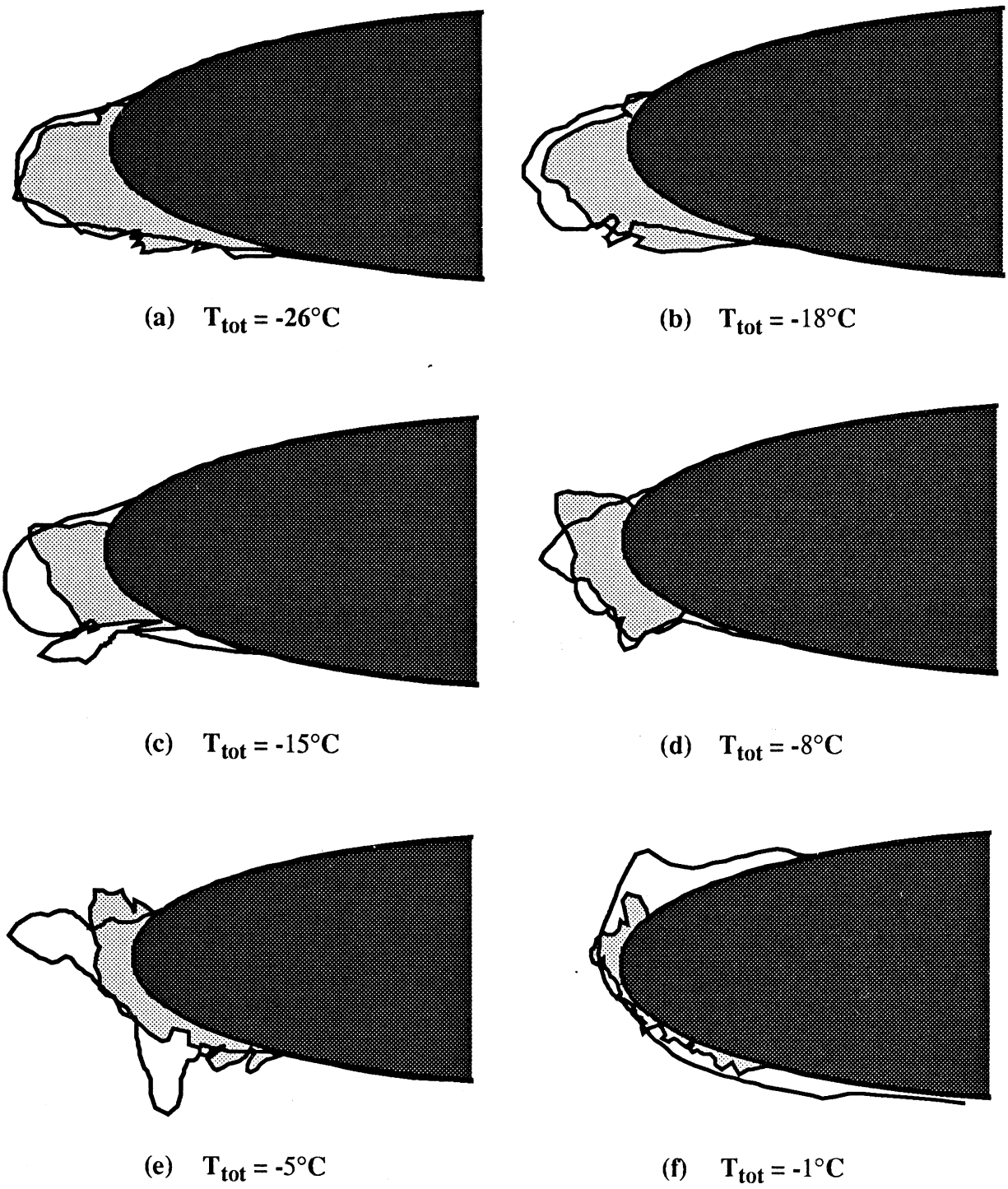

Figure 6 - Measured and calculated ice shapes for V=209 km/hr, LWC=1.3 g/m^3, MVD=20μm, Duration = 8min (except calculated (d) = 6min).

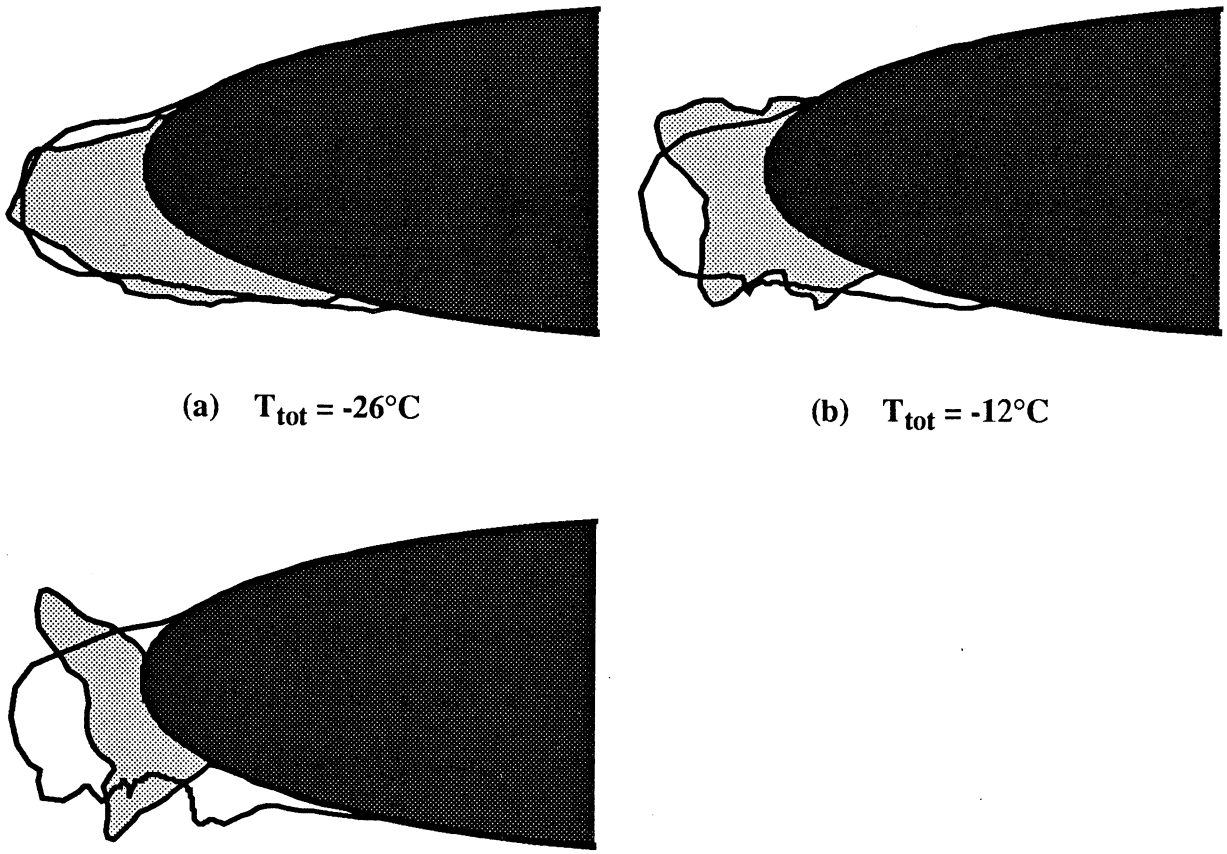

Figure 7 - Measured and calculated ice shapes for V=338 km/hr, LWC=1.05 g/m^3, MVD=20μm, Duration = 6.2min.

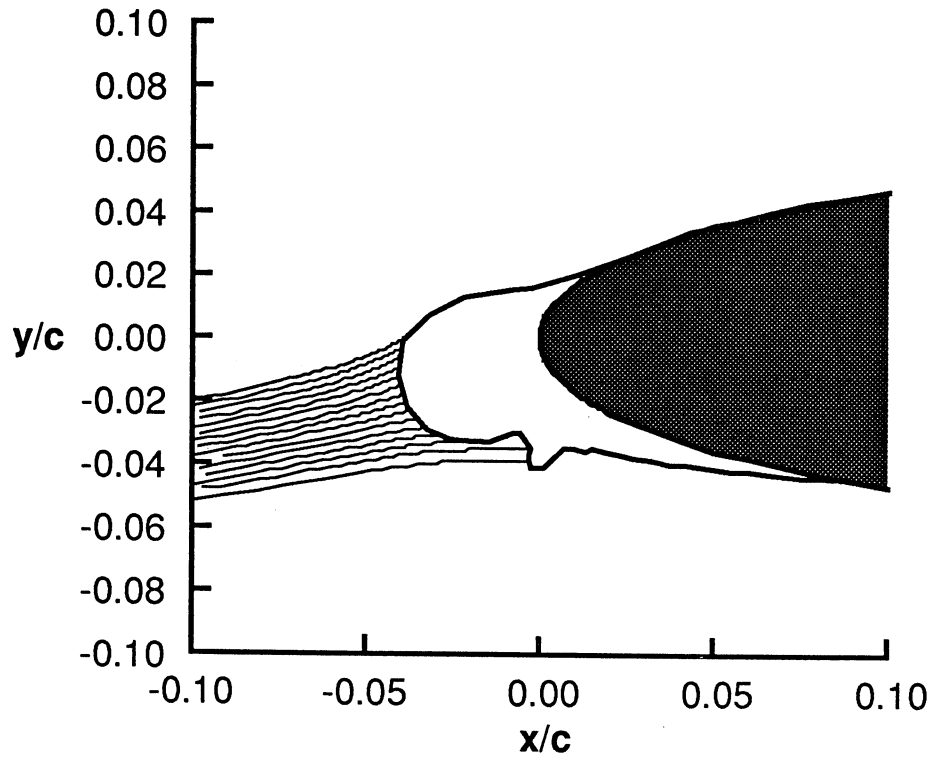

Figure 8 - Droplet trajectories from LEWICE/NS showing shadow region between main ice growth and horn.

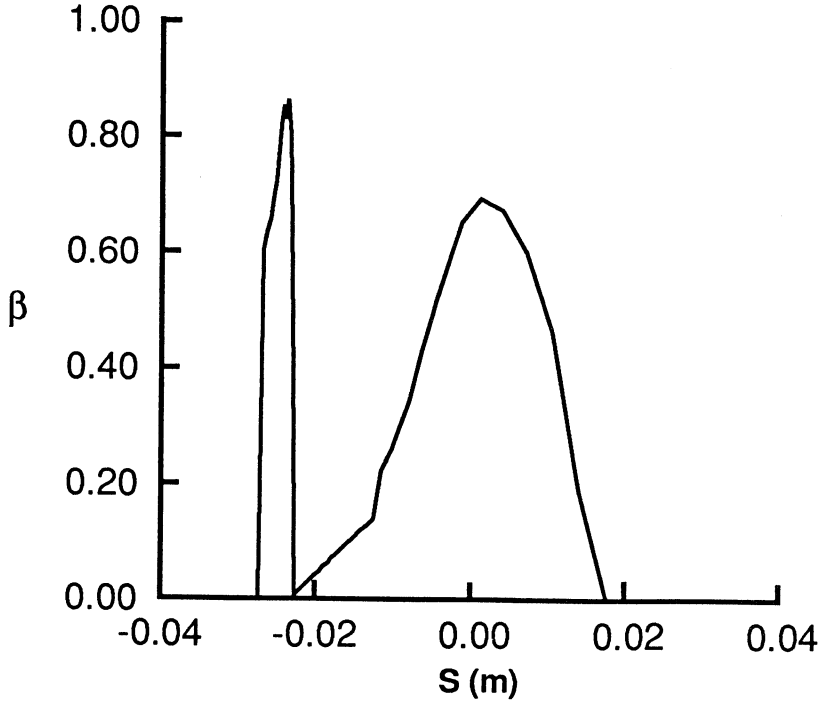

Figure 9 - Collection efficiency distribution resulting from droplet trajectories of Figure 8.

REPORT DOCUMENTATION PAGE

Form Approved
OMB No. 0704-0188

1. AGENCY USE ONLY (*Leave blank*)	2. REPORT DATE	3. REPORT TYPE AND DATES COVERED
	January 1993	Technical Memorandum

4. TITLE AND SUBTITLE

Ice Accretion and Performance Degradation Calculations with LEWICE/NS

5. FUNDING NUMBERS

WU–505–68–10–00

6. AUTHOR(S)

Mark G. Potapczuk, Kamel M. Al-Khalil, and Matthew T. Velazquez

7. PERFORMING ORGANIZATION NAME(S) AND ADDRESS(ES)

National Aeronautics and Space Administration
Lewis Research Center
Cleveland, Ohio 44135–3191

8. PERFORMING ORGANIZATION REPORT NUMBER

E–7497

9. SPONSORING/MONITORING AGENCY NAME(S) AND ADDRESS(ES)

National Aeronautics and Space Administration
Washington, DC 20546–0001

10. SPONSORING/MONITORING AGENCY REPORT NUMBER

NASA TM–105972
AIAA–93–0173

11. SUPPLEMENTARY NOTES

Prepared for the 31st Aerospace Sciences Meeting and Exhibit sponsored by the American Institute of Aeronautics and Astronautics, Reno, Nevada, January 11–14, 1993. Mark G. Potapczuk, NASA Lewis Research Center; Kamel M. Al-Khalil, National Research Council, Washington, DC 20418; and Matthew T. Velazquez, Massachusetts Institute of Technology, Cambridge, Massachusetts 02139. Responsible person, Mark. G. Potapczuk, 216–433–3919.

12a. DISTRIBUTION/AVAILABILITY STATEMENT

Unclassified - Unlimited
Subject Categories 02 and 03

This publication is available from the NASA Center for AeroSpace Information, (301) 621–0390.

12b. DISTRIBUTION CODE

13. ABSTRACT ***(Maximum 200 words)***

The LEWICE ice accretion computer code has been extended to include the solution of the two-dimensional Navier-Stokes equations. The code is modular and contains separate stand-alone program elements that create a grid, calculate the flow field parameters, calculate the droplet trajectory paths, determine the amount of ice growth, calculate aeroperformance changes, and plot results. The new elements of the code are described. Calculated results are compared to experiment for several cases, including both ice shape and drag rise.

14. SUBJECT TERMS

Aerodynamics; Aircraft icing

15. NUMBER OF PAGES

22

16. PRICE CODE

A03

17. SECURITY CLASSIFICATION OF REPORT	18. SECURITY CLASSIFICATION OF THIS PAGE	19. SECURITY CLASSIFICATION OF ABSTRACT	20. LIMITATION OF ABSTRACT
Unclassified	Unclassified	Unclassified	